

Synthesis and Crystal Structure Analysis of Histone Deacetylase Inhibitor Chidamide

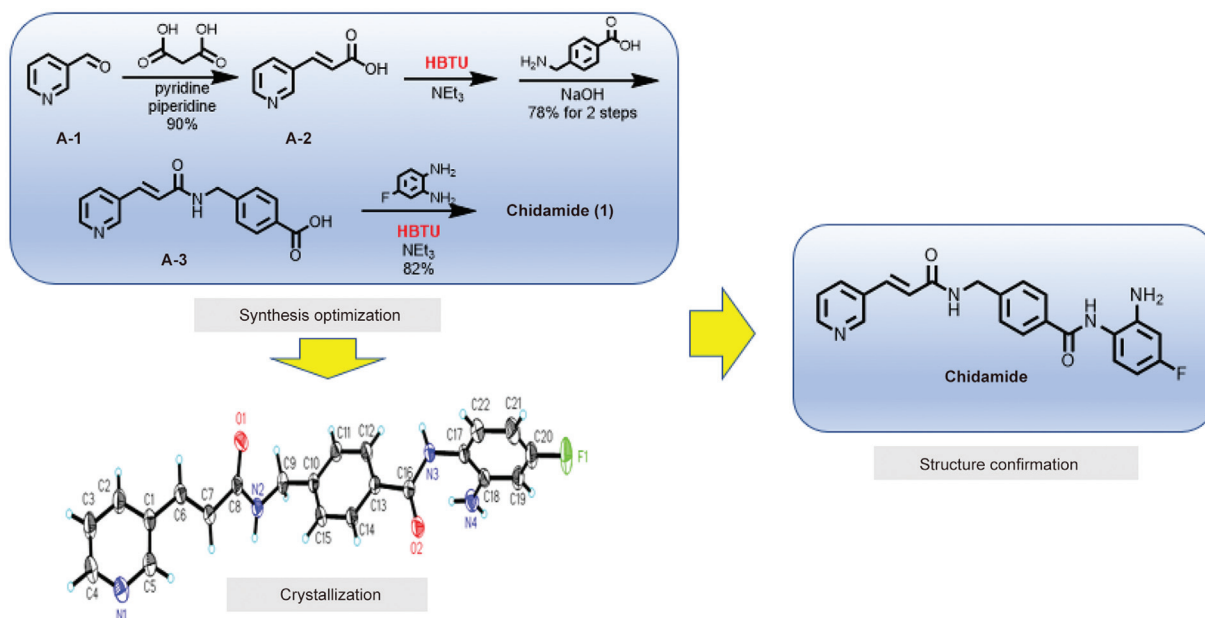
Bo Han^{1,#} Xin-Yan Peng^{1,#} Yan-Qing Gong² Jia-Liang Zhong² Qing-Wei Zhang^{1,*}

¹ Shanghai Institute of Pharmaceutical Industry Co., Ltd., China State Institute of Pharmaceutical Industry, Shanghai, People's Republic of China

² State Key Laboratory of New Drug and Pharmaceutical Process, Shanghai Institute of Pharmaceutical Industry Co., Ltd., China State Institute of Pharmaceutical Industry, Shanghai, People's Republic of China

Address for correspondence Qing-Wei Zhang, PhD, Novel Technology Center of Pharmaceutical Chemistry, Shanghai Institute of Pharmaceutical Industry Co., Ltd., 285 Gebaini Road, Shanghai 201203, People's Republic of China (e-mail: sipiqingwei@163.com).

Pharmaceut Fronts 2023;5:e91–e100.



Abstract

Chidamide is the first oral subtype-selective histone deacetylase inhibitor approved in China for the treatment of relapsed and refractory peripheral T cell lymphoma. Due to the existence of isomers, many articles or patents have mistaken its structure. Herein we explored the synthesis of the key intermediate (*E*)-4-((3-(pyridin-3-yl)acrylamido)methyl)benzoic acid (**A-3**) and chidamide, using the condensing agent HBTU, instead of the unstable *N,N'*-carbonyldiimidazole. The single crystal of chidamide was determined by X-ray diffraction study. The optimized preparation process was easy to operate, and the purity of the final product can be up to 99.76%. Moreover, the structure of chidamide was established to be (*E*)-*N*-(2-amino-4-fluorophenyl)-4-((3-(pyridin-3-yl)acrylamido)methyl)benzamide.

Keywords

- ▶ histone deacetylase
- ▶ chidamide
- ▶ synthesis
- ▶ HBTU
- ▶ single crystal

These authors contributed equally to this work.

received
September 3, 2022
accepted
March 31, 2023

DOI <https://doi.org/10.1055/s-0043-1768613>.
ISSN 2628-5088.

© 2023. The Author(s).

This is an open access article published by Thieme under the terms of the Creative Commons Attribution License, permitting unrestricted use, distribution, and reproduction so long as the original work is properly cited. (<https://creativecommons.org/licenses/by/4.0/>)
Georg Thieme Verlag KG, Rüdigerstraße 14, 70469 Stuttgart, Germany

Introduction

Chidamide (CS055, HBI-8000), a subtype-selective histone deacetylase (HDAC) inhibitor with oral antitumor activity, was discovered and developed by Chipscreen Biosciences and approved by the National Medical Products Administration (NMPA) in December 2014 for the treatment of relapsed or refractory peripheral T cell lymphoma.¹ In November 2019, a new indication of chidamide in combination with an aromatase inhibitor was approved by NMPA for the treatment of postmenopausal women with hormone receptor-positive, HER2-negative advanced breast cancer treated with endocrine therapies for recurrence or progression.² Chidamide was also approved by the Pharmaceuticals and Medical Devices Agency in 2021 for the treatment of relapsed or refractory (R/R) adult T cell leukemia-lymphoma.

The structure of chidamide is *N*-(2-amino-4-fluorophenyl)-4-(*N*-(*E*)-3-(pyridin-3-yl)acrylamido)methyl)benzamide (**1**) as reported by Chipscreen Biosciences. However, many articles or patents have also reported its structure as *N*-(2-amino-5-fluorophenyl)-4-(*N*-(*E*)-3-(pyridin-3-yl)acrylamido)methyl)benzamide (**2**), as shown in ►Fig. 1.^{3–13} The actual structure of chidamide has discrepancies, and this inconformity is mainly attributed to that both of the two amino groups on 4-fluorobenzene-1,2-diamine may participate in the reaction theoretically in the last step of acylation to produce chidamide (**1**) or its isomer (**2**).

Herein, we summarized and analyzed all the reported synthetic methods of chidamide and obtained chidamide by an optimized synthetic method. Meanwhile, the structure of chidamide was confirmed by single-crystal culture and X-ray single-crystal diffraction, and its molecular packing and intermolecular interactions in the crystalline state were described.

The Preparation of Chidamide

Currently, there are five synthetic methods of chidamide reported in patents or papers (►Fig. 2). *Method 1*: the synthesis was started with the acylation reaction between the activated (*E*)-3-(pyridin-3-yl)acrylic acid by *N,N'*-carbonyldiimidazole (CDI) and 4-(aminomethyl)benzoic acid under acidic conditions to afford the carboxylic acid intermediate, which was activated by CDI again and acylated with 4-fluorobenzene-1,2-diamine in the presence of trifluoroacetic acid to afford chidamide. The overall yield was 28%.¹⁴ *Method 2*: in this synthetic route, the carboxylic acid intermediate was obtained by the substitution reaction between (*E*)-3-(pyridin-3-yl)acrylamide and 4-(bromomethyl)benzoic acid. The carboxylic acid intermediate

was subjected to acylation with 4-fluorobenzene-1,2-diamine under acidic conditions to give a crude product, which was further purified by decolorization, thermal filtration, and acetone detrusion to obtain the target product with an overall yield of 68%. Nevertheless, the product obtained in the original paper was reported to be the isomer of chidamide.¹⁵ *Method 3*: the sequence began with the Knoevenagel condensation of nicotinaldehyde with malonic acid in a mixture of piperidine and pyridine. The obtained (*E*)-3-(pyridin-3-yl)acrylic acid was reacted with CDI and acylated with 4-(aminomethyl)benzoic acid to afford the carboxylic acid intermediate, which was activated by CDI again and treated with 4-fluorobenzene-1,2-diamine in the presence of trifluoroacetic acid, giving chidamide in 38% overall yields.¹⁶ *Method 4*: (*E*)-3-(pyridin-3-yl)acrylic acid was activated by CDI and subjected to the acylation reaction with 4-(aminomethyl)benzoic acid to afford the carboxylic acid intermediate, which was activated by 1-hydroxybenzotriazole (HOBT) under the catalytic conditions of dicyclohexyl carbimide (DCC) and reacted with 4-fluorobenzene-1,2-diamine to get chidamide in 62% overall yield.¹⁷ *Method 5*: methyl (*E*)-3-(pyridin-3-yl)acrylate was first prepared by the palladium acetate-catalyzed Heck reaction of 3-bromopyridine with methyl acrylate. Methyl (*E*)-3-(pyridin-3-yl)acrylate was then hydrolyzed to give (*E*)-3-(pyridin-3-yl)acrylic acid. After activation by CDI, this acrylic acid derivative was acylated with 4-(aminomethyl)benzoic acid to obtain the key amide-carboxylic acid intermediate. The 4-fluorobenzene-1,2-diamine used in the amidation reaction was obtained from the hydrogenation reduction of 4-fluoro-2-nitroaniline. Lastly, the carboxylic acid intermediate was activated by HBTU and DMAP (4-dimethylaminopyridine) and reacted with 4-fluorobenzene-1,2-diamine to get the target product with an overall yield of 87%.¹⁸

Despite the diversity of the published syntheses, the majority of them used (*E*)-3-(pyridin-3-yl)acrylic acid as the key intermediate, and then through two acylation reactions to give chidamide. In methods 1, 3, 4, and 5, CDI was used as the condensing agent in the reaction. However, the chemical properties of CDI are very active, and it is easy to form imidazole and carbon dioxide under atmospheric moisture, which would affect the process of the reaction and lead to the introduction of impurities. Therefore, these reactions required a strict anhydrous environment.¹⁹ Besides, the expensive (*E*)-3-(pyridin-3-yl)acrylamide was used as the starting material in method 2, and the process required careful temperature and pH control, which was not suitable for industrial process scale-up.



Fig. 1 Chemical structures of chidamide and its isomer.

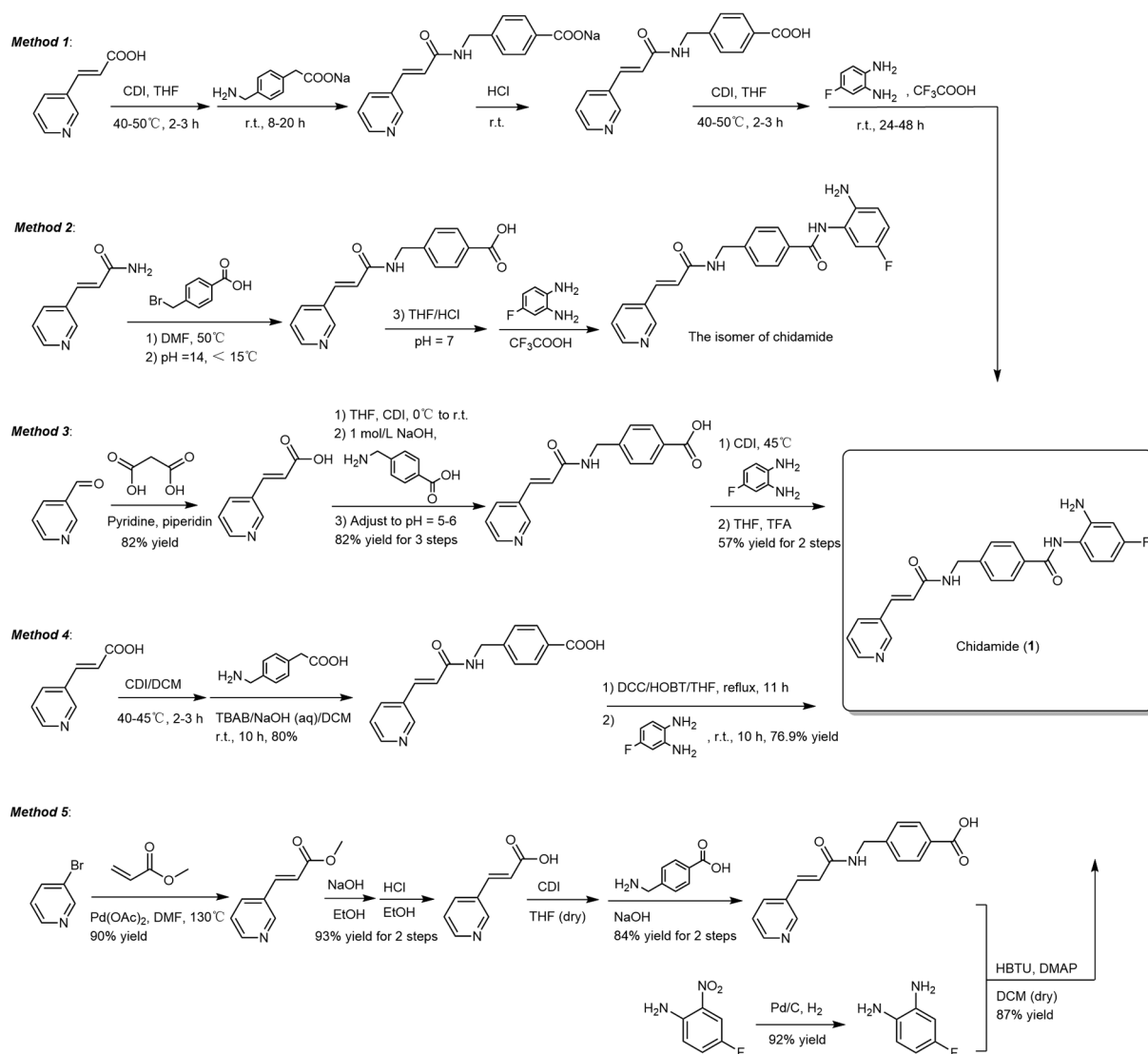


Fig. 2 Graphical synthetic routes to chidamide.

Inspired by method 3, we have optimized the synthetic route of chidamide. The sequence depicted in **Fig. 3** started with the Knoevenagel condensation reaction between nicotinaldehyde **A-1** and malonic acid in the mixture of piperidine and pyridine to afford (*E*)-3-(pyridin-3-yl) acrylic acid **A-2**. Acid **A-2** was then activated by HBTU and acylated with 4-(aminomethyl)benzoic acid to get the amide-acid **A-3**. Finally, chidamide was obtained by acylating **A-3** with 4-fluorobenzene-1,2-diamine. The overall reaction yield was 57.6%, much higher than that reported in method 3, and the high-performance liquid chromatography (HPLC) purity of the product was 99.76%. In the optimized synthesis route, HBTU was used as the condensing agent in the reaction, which avoided the harsh conditions required by CDI, simplified the experimental operation, and the reagents used were cheap and easy to obtain, and the whole reaction could obtain high-purity chidamide in high yield.

The Crystal Structure Analysis of Chidamide

The crystal structure analysis was performed according to Chinese Pharmacopoeia 2020 (Monographs Part IV General Chapters). One appropriate crystal was used to collect the diffraction data by CuK_α radiation in ϕ/ω scan mode. The total number of diffraction points was 6,626, including 2,940 independent diffraction points and 2,781 observable points ($|F|^2 \geq 2\sigma|F|^2$). The crystal structure was solved by the direct method and refined on F^2 by full-matrix least squares using the Shelxs-97 program package. All nonhydrogen atoms were refined anisotropically. All hydrogen atoms were added theoretically and the final reliable factors R_1 , wR_2 , and S were 0.0349, 0.0959, and 1.065, respectively.

The results of the single-crystal X-ray diffraction showed that the chemical formula of chidamide is C₂₂H₁₉FN₄O₂, the calculated molecular weight is 390.41, and the calculated density is 1.379 g/cm³. The chemical crystallizes in the

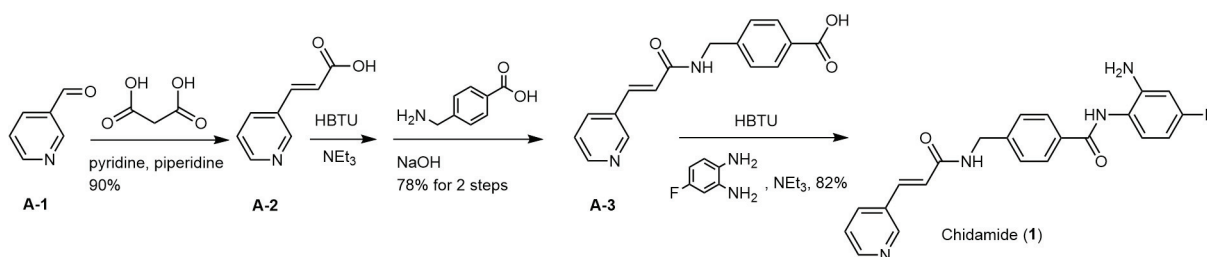


Fig. 3 The optimized synthetic route of chidamide.

monoclinic space group $P2_1$, with unit cell parameters $a = 8.8064(3)\text{\AA}$, $b = 5.1125(2)\text{\AA}$, $c = 20.8961(6)\text{\AA}$, $\alpha = \gamma = 90.00^\circ$, $\beta = 91.488(2)^\circ$. The volume of the unit cell is $940.48(6)\text{\AA}^3$. The absolute configuration diagram, the ORTEP diagram, and the cell stacking diagram extending along the b -axis are shown in ►Figs. 1, 4, and 5. The crystal data and structure refinement for chidamide are listed in ►Table 1, the atomic coordinates and equivalent isotropic displacement parameters for chidamide are given in ►Table 2, the bond lengths and angles for chidamide are listed in ►Table 3, the torsion angles for chidamide are shown in ►Table 4, and the hydrogen bonds are summarized in ►Table 5.

In the crystal structure of chidamide, the structural skeleton of chidamide comprises two benzene rings, one pyridine ring, and two sets of amide bonds. The dihedral angle between two benzene rings is 78.47° (almost vertical), the dihedral angle between the pyridine ring and terminal benzene ring is 81.88° (almost vertical), the dihedral angle between pyridine ring and middle benzene ring is 23.72° . In the crystalline state, there are hydrogen bonds between adjacent molecules. One molecule links to six adjacent molecules by hydrogen bonds: $N2-H2A\dots O2$ ($-x+2, y+1/2, -z$), $N3-H3A\dots O1$ ($-x+1, y+1/2, -z$), $N4-H4A\dots O2$ ($-x+2, y+3/2, -z$). The above-mentioned hydrogen bonds enhance the stable packing arrangement of molecules in the crystalline state, which is illustrated in the cell stacking diagram extending along the b -axis. CCDC 2208238 contains the supplementary crystallographic data for this article. The data can be obtained free of charge from the Cambridge Crystallographic Data Centre via www.ccdc.cam.ac.uk.

Result and Discussion

Herein we used HBTU as the condensation reagent to replace the unstable and hygroscopic CDI, and optimized the reaction temperature, reaction time, and reaction operation. The improved preparation process was simple and convenient, which could obtain chidamide with high purity. The X-ray single-crystal diffraction analysis is the most intuitive method for determining the absolute configuration of a compound, and we further cultivated single crystals of chidamide by the solvent evaporation method and used X-ray single-crystal diffraction to analyze and confirm its actual structure. The results showed that the crystal belongs to the monoclinic crystal system, and each molecule has intermolecular hydrogen bonds with six adjacent molecules, which enhances the stable arrangement in space. The absolute configuration of chidamide can be intuitively solved by the crystal structure solution.

To further explain the regional selectivity between the two amino groups residing on the benzene ring in the process of synthesis, we can compare the nucleophilicity of the two amino groups residing on the benzene ring. The fluorine atom's electron-withdrawing induction has a weaker effect at the delocalized lone pair of *para*- NH_2 than that of the *meta*- NH_2 as a result of interaction distance. On the other side, the p - π conjugation of the lone pairs on fluorine with the benzene ring would increase the amino groups' electron density in the *ortho*- and *para*-positions. Consequently, the amino group on the *para*-position should be more nucleophilic than the *meta*-amino group, and is easier to attack HBTU as a nucleophile. Both of electron donation by conjugation and electron withdrawal by

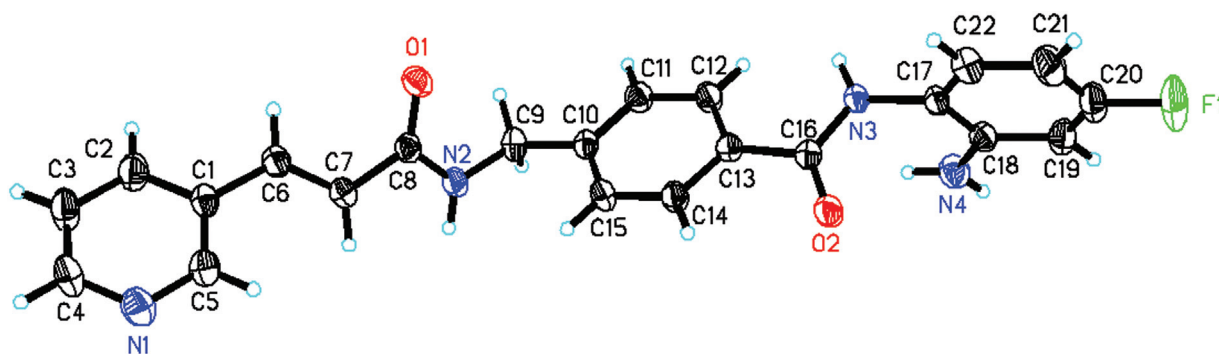


Fig. 4 ORTEP diagram of chidamide.

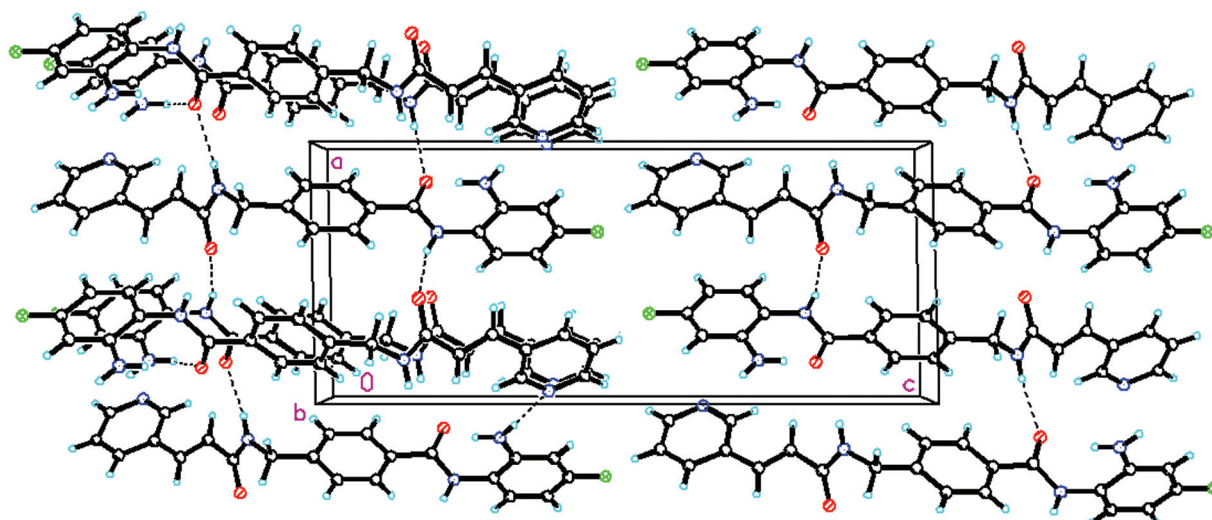


Fig. 5 The cell stacking diagram extending along the *b*-axis.

Table 1 Crystal data and structure refinement for chidamide

Project	Crystal date	
Chemical formula	C ₂₂ H ₁₉ FN ₄ O ₂	
Formula weight	390.41	
Temperature	296(2) K	
Wavelength	1.54178 Å	
Crystal system, space group	Monoclinic, <i>P</i> 2 ₁	
Unit cell dimensions	<i>a</i> = 8.8064(3) Å <i>b</i> = 5.1125(2) Å <i>c</i> = 20.8961(6) Å	$\alpha = 90^\circ$ $\beta = 91.488(2)^\circ$ $\gamma = 90^\circ$
Cell volume	940.48(6) Å ³	
<i>Z</i> , calculated density	2, 1.379 g/cm ³	
Absorption coefficient	0.806 mm ⁻¹	
<i>F</i> (000)	408	
Crystal size	0.30 × 0.04 × 0.03 mm	
Theta range for data collection	2.11–68.14°	
Limiting indices of <i>hkl</i>	−14 ≤ <i>h</i> ≤ 10, −5 ≤ <i>k</i> ≤ 5, −24 ≤ <i>l</i> ≤ 23	
Reflections collected/unique	6626/2940 [<i>R</i> (int) = 0.0230]	
Completeness to theta = 68.14	95.7%	
Absorption correction	Semi-empirical from equivalents	
Max. and min. transmission	0.7530 and 0.6240	
Refinement method	Full-matrix least-squares on <i>F</i> ²	
Data/restraints/parameters	2940/1/262	
Goodness-of-fit on <i>F</i> ²	1.065	
Final <i>R</i> indices [<i>I</i> > 2σ(<i>I</i>)]	<i>R</i> ₁ = 0.0349, <i>wR</i> ₂ = 0.0349	
<i>R</i> indices (all data)	<i>R</i> ₁ = 0.0371, <i>wR</i> ₂ = 0.0349	
Absolute structure parameter	0.0 (2)	
Largest diff. peak and hole	0.165 and −0.203 e.Å ⁻³	

Table 2 Atomic coordinates ($\times 10^4$) and equivalent isotropic displacement parameters ($\text{\AA}^2 \times 10^3$) for chidamide

Atoms	x	y	z	U(eq)
F(1)	6617(2)	6479(5)	4589(1)	105(1)
O(1)	5962(2)	7037(3)	-1737(1)	57(1)
O(2)	8580(2)	5774(4)	1787(1)	62(1)
N(1)	9622(2)	-189(4)	-3710(1)	65(1)
N(2)	8230(2)	8860(4)	-1514(1)	48(1)
N(3)	6575(2)	8342(4)	1992(1)	48(1)
N(4)	8397(2)	11339(4)	2832(1)	61(1)
C(1)	7949(2)	3240(4)	-3376(1)	49(1)
C(2)	7373(3)	3460(6)	-3997(1)	65(1)
C(3)	7942(3)	1867(6)	-4466(1)	74(1)
C(4)	9041(3)	79(6)	-4303(1)	69(1)
C(5)	9075(2)	1395(5)	-3263(1)	55(1)
C(6)	7335(2)	4828(4)	-2855(1)	50(1)
C(7)	8071(2)	5574(4)	-2329(1)	48(1)
C(8)	7329(2)	7180(4)	-1839(1)	44(1)
C(9)	7625(3)	10699(4)	-1059(1)	51(1)
C(10)	7558(2)	9692(4)	-377(1)	42(1)
C(11)	6691(2)	11035(4)	55(1)	49(1)
C(12)	6661(2)	10320(4)	693(1)	50(1)
C(13)	7520(2)	8194(4)	911(1)	43(1)
C(14)	8374(2)	6837(4)	477(1)	47(1)
C(15)	8398(2)	7573(4)	-160(1)	47(1)
C(16)	7598(2)	7336(4)	1597(1)	45(1)
C(17)	6600(2)	7820(4)	2667(1)	45(1)
C(18)	7493(2)	9412(4)	3068(1)	48(1)
C(19)	7474(3)	8916(5)	3727(1)	60(1)
C(20)	6608(3)	6909(6)	3946(1)	66(1)
C(21)	5746(3)	5317(6)	3565(1)	68(1)
C(22)	5748(3)	5811(5)	2911(1)	58(1)
H(2A)	9191	8845	-1578	58
H(3A)	5875	9342	1835	58
H(3B)	8426	11599	2426	73
H(4A)	8936	12293	3089	73
H(4B)	6613	4668	-4097	78
H(2B)	7583	2005	-4887	88
H(3B)	9402	-1006	-4622	83
H(4C)	9477	1249	-2849	66
H(5A)	6328	5358	-2902	60
H(6A)	9079	5078	-2265	58
H(7A)	6607	11188	-1201	61
H(9A)	8244	12267	-1060	61
H(9B)	6113	12453	-87	59
H(11A)	6070	11255	976	60
H(12A)	8943	5402	615	56

Table 2 (Continued)

Atoms	x	y	z	U(eq)
H(14A)	8983	6634	-444	56
H(15A)	8044	9941	4012	72
H(19A)	5181	3957	3733	81
H(21A)	5746(3)	5317(6)	3565(1)	68(1)

Table 3 Relevant bond lengths and angles for chidamide

Bonding atoms	Bond length/(Å)	Bonding atoms	Bond angle/(°)	Bonding atoms	Bond angle/(°)
F(1)-C(20)	1.361(2)	C(5)-N(1)-C(4)	116.8(2)	C(14)-C(13)-C(16)	117.99(17)
O(1)-C(8)	1.230(2)	C(8)-N(2)-C(9)	121.66(17)	C(12)-C(13)-C(16)	123.44(17)
O(2)-C(16)	1.234(2)	C(8)-N(2)-H(2A)	119.2	C(13)-C(14)-C(15)	121.18(18)
N(1)-C(5)	1.335(3)	C(9)-N(2)-H(2A)	119.2	C(13)-C(14)-H(14A)	119.4
N(1)-C(4)	1.337(3)	C(16)-N(3)-C(17)	122.71(16)	C(15)-C(14)-H(14A)	119.4
N(2)-C(8)	1.342(3)	C(16)-N(3)-H(3A)	118.6	C(10)-C(15)-C(14)	120.46(18)
N(2)-C(9)	1.450(3)	C(17)-N(3)-H(3A)	118.6	C(10)-C(15)-H(15A)	119.8
N(2)-H(2A)	0.8600	C(18)-N(4)-H(4A)	120.0	C(14)-C(15)-H(15A)	119.8
N(3)-C(16)	1.340(3)	C(18)-N(4)-H(4B)	120.0	O(2)-C(16)-N(3)	121.81(18)
N(3)-C(17)	1.435(2)	H(4A)-N(4)-H(4B)	120.0	O(2)-C(16)-C(13)	120.69(18)
N(3)-H(3A)	0.8600	C(5)-C(1)-C(2)	117.2(2)	N(3)-C(16)-C(13)	117.50(17)
N(4)-C(18)	1.366(3)	C(5)-C(1)-C(6)	121.72(18)	C(22)-C(17)-C(18)	121.14(18)
N(4)-H(4A)	0.8600	C(2)-C(1)-C(6)	121.0(2)	C(22)-C(17)-N(3)	120.49(19)
N(4)-H(4B)	0.8600	C(3)-C(2)-C(1)	119.1(2)	C(18)-C(17)-N(3)	118.37(19)
C(1)-C(5)	1.384(3)	C(3)-C(2)-H(2B)	120.4	N(4)-C(18)-C(17)	121.90(18)
C(1)-C(2)	1.387(3)	C(1)-C(2)-H(2B)	120.4	N(4)-C(18)-C(19)	120.5(2)
C(1)-C(6)	1.472(3)	C(4)-C(3)-C(2)	119.1(2)	C(17)-C(18)-C(19)	117.6(2)
C(2)-C(3)	1.378(4)	C(4)-C(3)-H(3B)	120.4	C(20)-C(19)-C(18)	119.1(2)
C(2)-H(2B)	0.9300	C(2)-C(3)-H(3B)	120.4	C(20)-C(19)-H(19A)	120.4
C(3)-C(4)	1.368(4)	N(1)-C(4)-C(3)	123.4(2)	C(18)-C(19)-H(19A)	120.4
C(3)-H(3B)	0.9300	N(1)-C(4)-H(4C)	118.3	C(21)-C(20)-F(1)	118.1(2)
C(4)-H(4C)	0.9300	C(3)-C(4)-H(4C)	118.3	C(21)-C(20)-C(19)	124.3(2)
C(5)-H(5A)	0.9300	N(1)-C(5)-C(1)	124.37(19)	F(1)-C(20)-C(19)	117.6(2)
C(6)-C(7)	1.318(3)	N(1)-C(5)-H(5A)	117.8	C(20)-C(21)-C(22)	117.0(2)
C(6)-H(6A)	0.9300	C(1)-C(5)-H(5A)	117.8	C(20)-C(21)-H(21A)	121.5
C(7)-C(8)	1.477(3)	C(7)-C(6)-C(1)	126.42(19)	C(22)-C(21)-H(21A)	121.5
C(7)-H(7A)	0.9300	C(7)-C(6)-H(6A)	116.8	C(17)-C(22)-C(21)	120.9(2)
C(9)-C(10)	1.518(3)	C(1)-C(6)-H(6A)	116.8	C(17)-C(22)-H(22A)	119.5
C(9)-H(9A)	0.9700	C(6)-C(7)-C(8)	121.44(18)	C(21)-C(22)-H(22A)	119.5
C(9)-H(9B)	0.9700	C(6)-C(7)-H(7A)	119.3		
C(10)-C(11)	1.379(3)	C(8)-C(7)-H(7A)	119.3		
C(10)-C(15)	1.381(3)	O(1)-C(8)-N(2)	121.23(18)		
C(11)-C(12)	1.385(3)	O(1)-C(8)-C(7)	122.65(18)		
C(11)-H(11A)	0.9300	N(2)-C(8)-C(7)	116.10(17)		
C(12)-C(13)	1.394(3)	N(2)-C(9)-C(10)	114.90(18)		
C(12)-H(12A)	0.9300	N(2)-C(9)-H(9A)	108.5		

(Continued)

Table 3 (Continued)

Bonding atoms	Bond length/(Å)	Bonding atoms	Bond angle/(°)	Bonding atoms	Bond angle/(°)
C(13)-C(14)	1.381(3)	C(10)-C(9)-H(9A)	108.5		
C(13)-C(16)	1.499(3)	N(2)-C(9)-H(9B)	108.5		
C(14)-C(15)	1.383(3)	C(10)-C(9)-H(9B)	108.5		
C(14)-H(14A)	0.9300	H(9A)-C(9)-H(9B)	107.5		
C(15)-H(15A)	0.9300	C(11)-C(10)-C(15)	118.51(17)		
C(17)-C(22)	1.377(3)	C(11)-C(10)-C(9)	118.70(18)		
C(17)-C(18)	1.396(3)	C(15)-C(10)-C(9)	122.69(17)		
C(18)-C(19)	1.402(3)	C(10)-C(11)-C(12)	121.54(18)		
C(19)-C(20)	1.365(4)	C(10)-C(11)-H(11A)	119.2		
C(19)-H(19A)	0.9300	C(12)-C(11)-H(11A)	119.2		
C(20)-C(21)	1.357(4)	C(11)-C(12)-C(13)	119.75(18)		
C(21)-C(22)	1.390(3)	C(11)-C(12)-H(12A)	120.1		
C(21)-H(21A)	0.9300	C(13)-C(12)-H(12A)	120.1		
C(22)-H(22A)	0.9300	C(14)-C(13)-C(12)	118.55(17)		

Table 4 Torsion angles for chidamide

Connecting atoms	Torsion Angle/(°)	Connecting atoms	Torsion Angle/(°)
C(5)-C(1)-C(2)-C(3)	-0.2 (4)	C(16)-C(13)-C(14)-C(15)	-177.79 (19)
C(6)-C(1)-C(2)-C(3)	-177.6 (2)	C(11)-C(10)-C(15)-C(14)	-0.5 (3)
C(1)-C(2)-C(3)-C(4)	1.1 (4)	C(9)-C(10)-C(15)-C(14)	175.74 (19)
C(5)-N(1)-C(4)-C(3)	0.2 (4)	C(13)-C(14)-C(15)-C(10)	-0.2 (3)
C(2)-C(3)-C(4)-N(1)	-1.1 (5)	C(17)-N(3)-C(16)-O(2)	4.1 (3)
C(4)-N(1)-C(5)-C(1)	0.8 (4)	C(17)-N(3)-C(16)-C(13)	-175.43 (18)
C(2)-C(1)-C(5)-N(1)	-0.8 (3)	C(14)-C(13)-C(16)-O(2)	12.0 (3)
C(6)-C(1)-C(5)-N(1)	176.5 (2)	C(12)-C(13)-C(16)-O(2)	-166.4 (2)
C(5)-C(1)-C(6)-C(7)	30.2 (3)	C(14)-C(13)-C(16)-N(3)	-168.44 (19)
C(2)-C(1)-C(6)-C(7)	-152.5 (2)	C(12)-C(13)-C(16)-N(3)	13.1 (3)
C(1)-C(6)-C(7)-C(8)	179.8 (2)	C(16)-N(3)-C(17)-C(22)	-93.8 (3)
C(9)-N(2)-C(8)-O(1)	-4.1 (3)	C(16)-N(3)-C(17)-C(18)	86.8 (3)
C(9)-N(2)-C(8)-C(7)	174.88 (17)	C(22)-C(17)-C(18)-N(4)	177.1 (2)
C(6)-C(7)-C(8)-O(1)	31.0 (3)	N(3)-C(17)-C(18)-N(4)	-3.6 (3)
C(6)-C(7)-C(8)-N(2)	-148.0 (2)	C(22)-C(17)-C(18)-C(19)	-0.9 (3)
C(8)-N(2)-C(9)-C(10)	90.0 (2)	N(3)-C(17)-C(18)-C(19)	178.41 (18)
N(2)-C(9)-C(10)-C(11)	-165.17 (18)	N(4)-C(18)-C(19)-C(20)	-177.3 (2)
N(2)-C(9)-C(10)-C(15)	18.6 (3)	C(17)-C(18)-C(19)-C(20)	0.7 (3)
C(15)-C(10)-C(11)-C(12)	0.7 (3)	C(18)-C(19)-C(20)-C(21)	0.2 (4)
C(9)-C(10)-C(11)-C(12)	-175.72 (19)	C(18)-C(19)-C(20)-F(1)	179.9 (2)
C(10)-C(11)-C(12)-C(13)	-0.2 (3)	F(1)-C(20)-C(21)-C(22)	179.5 (2)
C(11)-C(12)-C(13)-C(14)	-0.6 (3)	C(19)-C(20)-C(21)-C(22)	-0.7 (4)
C(11)-C(12)-C(13)-C(16)	177.9 (2)	C(18)-C(17)-C(22)-C(21)	0.3 (3)
C(12)-C(13)-C(14)-C(15)	0.7 (3)	N(3)-C(17)-C(22)-C(21)	-179.0 (2)
C(2)-C(1)-C(7)-C(8)	0.5 (2)	C(20)-C(21)-C(22)-C(17)	0.5 (4)
C(6)-C(1)-C(7)-C(8)	179.45 (15)		

Table 5 Hydrogen bonds for chidamide

Donor-H...acceptor	d(D-H)	d(H...A)	d(D...A)	<(DHA)
N(2)-H(2A)...O(2)#1	0.86	2.25	3.043 (2)	153.3
N(3)-H(3A)...O(1)#2	0.86	2.13	2.964 (2)	163.0
N(4)-H(4B)...N(1)#3	0.86	2.21	3.065 (3)	177.2
N(4)-H(4A)...O(2)#4	0.86	2.52	3.155 (3)	131.0

Note: Symmetry transformations used to generate equivalent atoms:

#1 $-x+2, y+1/2, -z$.

#2 $-x+1, y+1/2, -z$.

#3 $-x+2, y+3/2, -z$.

#4 $x, y+1, z$.

induction make 4-fluorobenzene-1,2-diamine react regioselectively with **A3**, leading to the formation of chidamide.

Conclusion

Chidamide is a first-in-class orally active benzamide class of HDAC inhibitors approved in China and Japan for treating tumor diseases and has achieved good clinical efficacy. As an approved drug, the actual structure of chidamide is uncertain and the main reason is that two amine groups on 1,2-diamino-4-fluorobenzene can participate in the acylation reaction theoretically to produce chidamide or its isomer. It is necessary and interesting to confirm the absolute structure of chidamide. First we successfully obtained chidamide with high purity using an optimized preparation method. Based on X-ray single-crystal diffraction as the most intuitive method for determining the absolute configuration of a compound, we further obtained single crystals of chidamide by a solvent evaporation method. The results of X-ray single-crystal diffraction confirmed that the absolute configuration of chidamide is (*E*)-*N*-(2-amino-4-fluorophenyl)-4-((3-(pyridin-3-yl)acrylamido)methyl)benzamide. Meanwhile, we speculated on the reaction mechanism of regional selectivity from the point of view of the conjugation and induction, which further provided theoretical support for confirming the absolute structure of chidamide.

Experimental Section

Instruments and Reagents

Unless otherwise noted, all solvents and reagents were commercially available (Bidepharm, Shanghai, People's Republic of China) and used without further purification. All reactions were monitored by thin-layer chromatography (TLC) on 0.25 mm silica gel plates (60 GF-254) and visualized with ultraviolet light (Shanghai Heqi Glassware Co., Ltd., People's Republic of China). ¹H-NMR and ¹³C-NMR spectra were obtained using a Bruker DRX spectrometer (Bruker Co., Ettlingen, Germany) at 600 and 150 MHz. The melting point was measured with a WRS-2A microcomputer melting point apparatus (Shanghai INESA Physico-optical Instrument Co., Ltd.) without the calibration of the thermometer.

Electrospray ionization mass spectrometry (ESI-MS) was determined on an API 4000 spectrometer (Applied Biosystems, Foster City, California, United States) with a turbo ion spray interface. HPLC analysis was performed on Agilent 1200 (Agilent Technologies, California, United States) with an extended C18 column (4.6 mm × 250 mm, 5 μm). Single-crystal diffraction experiment was performed using a Bruker SMART APEX-II single crystal X-ray diffractometer (Bruker AXS Co., Germany).

Synthesis Experiment

Procedure for the Preparation of (*E*)-3-(pyridin-3-yl)acrylic acid (**A-2**)

The sequence began with the condensation of nicotinaldehyde (**A-1**, 5.36 g, 50 mmol) and malonic acid (5.20 g, 50 mmol) in a mixture of piperidine (3.96 g, 50 mmol) and pyridine (0.5 ml), and refluxed at 110°C for 2.5 hours. After the reaction completion shown by TLC, the mixture was cooled to room temperature and poured into 200 mL water. Adjusting the pH of the solution to 5 with hydrochloric acid (1 mol/L), whereby a white precipitate was formed which was then dried to get **A-2** (6.71 g, 90% yield, 97% HPLC purity). mp: 231.6–233.2°C ESI-MS (*m/z*): calcd. for [M+H]⁺ 150.0477; found 149.90. ¹H-NMR (600 Hz, DMSO-*d*₆) δ 12.57 (s, 1H), 8.86 (d, *J*=2.2 Hz, 1H), 8.59 (dd, *J*=4.8, 1.6 Hz, 1H), 8.16 (dt, *J*=7.9, 2.0 Hz, 1H), 7.64 (d, *J*=16.1 Hz, 1H), 7.45 (dd, *J*=8.0, 4.8 Hz, 1H), 6.69 (d, *J*=16.1 Hz, 1H).

Procedure for the Preparation of (*E*)-4-((3-(pyridin-3-yl)acrylamido)methyl)benzoic acid (**A-3**)

To a solution of **A-2** (7.45 g, 50 mmol) in DMF were added HBTU (18.95 g, 50 mmol), and triethylamine (10.1 g, 100 mmol) dropwise at 0°C. After the mixture was stirred at room temperature for 1 hour, 4-(aminomethyl)benzoic acid dissolved in 50 mL of 1 mol/L sodium hydroxide solution was added dropwise to the reaction solution and stirred for 4 hours. After the reaction was complete as shown by TLC, the pH of the solution was adjusted to 6 with concentrated hydrochloric acid to afford a white solid of **A-3** (11.0 g, 78% yield, 99.75% HPLC purity). mp: 248.8–251.4°C. ESI-MS (*m/z*): calcd. for [M+H]⁺ 283.1004; found 283.00. ¹H-NMR

(600 Hz, DMSO- d_6) δ 12.90 (s, 1H), 8.87–8.68 (m, 2H), 8.56 (dd, J = 4.8, 1.6 Hz, 1H), 8.01 (dt, J = 8.0, 2.0 Hz, 1H), 7.97–7.85 (m, 2H), 7.53 (d, J = 15.9 Hz, 1H), 7.48–7.30 (m, 3H), 6.82 (d, J = 15.9 Hz, 1H), 4.49 (d, J = 6.0 Hz, 2H).

Procedure for the Preparation of (*E*)-*N*-(2-amino-4-fluorophenyl)-4-((3-(pyridin-3-yl)acrylamido)methyl)benzamide (chidamide)

To the solution of **A-3** (0.282 g, 1 mmol), 4-fluorobenzene-1,2-diamine (0.139 g, 1.1 mmol), HBTU (0.455 g, 1.2 mmol) in DMF (5 mL) was added triethylamine dropwise, then the mixture was stirred at room temperature for 4 hours (monitored by TLC). After the completion of the reaction, water was added to precipitate a white solid. The solid was separated by Buchner funnel filtration and washed with saturated sodium bicarbonate solution, saturated sodium chloride solution, and water and recrystallized from 95% ethanol to afford the desired chidamide (0.32 g, 82% yield, 99.76% HPLC purity). mp: 164.3–166.8°C ESI-MS (m/z): calcd. for $[M+H]^+$ 391.1492; found 391.00. $^1\text{H-NMR}$ (600 MHz, DMSO- d_6) δ 9.50 (s, 1H), 8.77 (d, J = 2.0 Hz, 1H), 8.55 (dd, J = 1.6 Hz, 4.8 Hz, 1H), 7.98 (m, 3H), 7.95 (t, J = 5.6 Hz, 1H), 7.41–7.55 (m, 4H), 7.12 (t, J = 6.4 Hz, 1H), 6.82 (d, J = 16 Hz, 1H), 6.55 (dd, J = 2.8, 11.2 Hz, 1H), 6.35 (td, J = 2.8 Hz, 8.4 Hz, 1H), 5.16 (s, 2H), 4.49 (d, J = 6.0 Hz, 2H). $^{13}\text{C-NMR}$ (150 MHz, DMSO- d_6) δ 165.85, 165.15, 162.29, 160.70, 150.67, 149.64, 145.94, 143.36, 136.31, 134.47, 133.58, 131.12, 129.03, 128.38, 127.56, 124.42, 119.74, 102.59, 102.44, 102.02, 101.85, 42.57.

Single Crystal Growth Experiment

Single crystal culture of chidamide was performed using a solvent evaporation method. The above-prepared chidamide (30 mg, 0.077 mmol) was dissolved in 10 mL methanol and filtered the solution, then the filtrate was poured into a 25 mL beaker, then let it naturally volatilize at room temperature for 2 weeks to obtain the single crystal of chidamide.

Funding

We gratefully acknowledge financial support from the National Science and Technology Major Project (Grant No. 2018ZX09711002-002-009), the National Natural Science Foundation of China (Grant No. 81703358), Science and Technology Commission of Shanghai Municipality (Grant No. 17431903900, 18QB1404200, 21S11908000, and 22ZR1460300), and Graduate Innovation Fund Project of China State Institute of Pharmaceutical Industry (Grant No. YJS2021013 and YJS2021011).

Conflict of Interest

The authors declare no conflict of interest.

References

- Pan DS, Yang QJ, Fu X, et al. Discovery of an orally active subtype-selective HDAC inhibitor, chidamide, as an epigenetic modulator for cancer treatment. *MedChemComm* 2014;5(12):1789–1796
- Jiang Z, Li W, Hu X, et al. Tucidinostat plus exemestane for postmenopausal patients with advanced, hormone receptor-positive breast cancer (ACE): a randomised, double-blind, placebo-controlled, phase 3 trial. *Lancet Oncol* 2019;20(06):806–815
- Baldino CM, Muollo L, Warner JC, et al. Non-covalent derivatives and methods of treatment. WO Patent 2018222572 A1. December, 2018
- Cuadrado T, María dM, García O, et al. Products for the treatment and prevention of neurological disorders coursing with a cognition deficit or impairment, and of neurodegenerative diseases. WO Patent 2016030345 A1. March, 2016
- Chi LN, Yuan Y, Zhou FK, et al. Patent analysis of HDAC inhibitor chidamide [in Chinese]. *Chin J New Drug* 2020;29(01):15–21
- Liu L, Chen B, Qin S, et al. A novel histone deacetylase inhibitor Chidamide induces apoptosis of human colon cancer cells. *Biochem Biophys Res Commun* 2010;392(02):190–195
- Nepali K, Chang TY, Lai MJ, et al. Purine/purine isoster based scaffolds as new derivatives of benzamide class of HDAC inhibitors. *Eur J Med Chem* 2020;196:112291
- Singh A, Chang TY, Kaur N, et al. CAP rigidification of MS-275 and chidamide leads to enhanced antiproliferative effects mediated through HDAC1, 2 and tubulin polymerization inhibition. *Eur J Med Chem* 2021;215:113169
- Wu YF, Ou CC, Chien PJ, Chang HY, Ko JL, Wang BY. Chidamide-induced ROS accumulation and miR-129-3p-dependent cell cycle arrest in non-small lung cancer cells. *Phytomedicine* 2019;56:94–102
- Yuan XG, Huang YR, Yu T, Jiang HW, Xu Y, Zhao XY. Chidamide, a histone deacetylase inhibitor, induces growth arrest and apoptosis in multiple myeloma cells in a caspase-dependent manner. *Oncol Lett* 2019;18(01):411–419
- Zhu X, Zhang J, Sun Y, et al. Restoration of miR-23a expression by chidamide sensitizes CML cells to imatinib treatment with concomitant downregulation of CRYAB. *Bioengineered* 2022;13(04):8881–8892
- Li JY, Xu WT, Zhuo R, et al. The research progress of chidamide antitumor mechanism [in Chinese]. *Zhongliu Yaoxue* 2019;9(01):6–925
- Yin ZH, Wu ZW, Lan YK, et al. Synthesis of chidamide, a new histone deacetylase (HDAC) inhibitor [in Chinese]. *Chin J New Drug* 2004;13(06):536–538
- Lu XP, Li ZB, Xu XK. E-configuration benzamide compound and pharmaceutical formulation and application thereof. WO Patent 2015149435 A1. October, 2015
- Liu HZ, Ma JL, Guan CT, Guo M. A synthetic method of chidamide (in Chinese). CN Patent 105949114 A. September, 2016
- Flick AC, Ding HX, Leverett CA, et al. Synthetic approaches to the 2014 new drugs. *Bioorg Med Chem* 2016;24(09):1937–1980
- Zhao JH, Hu H, Guan Y, Liao F, Yu XH. Process optimization of chidamide [in Chinese]. *Carol J Pharm* 2017;48(07):994–996
- Zhang LH, Zhu RY, Wei CF, Liu XT, Yu XH. Study on the synthetic process of chidamide [in Chinese]. *Zhongguo Yaowu Huaxue Zazhi* 2021;31(08):589–592
- Engstrom KM, Sheikh A, Ho R, et al. The stability of *N,N*-carbonyldiimidazole toward atmospheric moisture. *Org Process Res Dev* 2014;18(04):488–494